Supplementary Information

Robust Photo-electrochemical route for the ambient fixation of di-nitrogen into ammonia over nanojunction assembled from ceria and iron boride/phosphide co-catalyst

S. Sultana, L. Paramanik, S. Mansingh and K. M. Parida *

Centre for Nano Science and Nano Technology, SOA Deemed to be University, Bhubaneswar—751 030, Odisha (India)

*Corresponding author

E-mail: paridakulamani@yahoo.com &

kulamaniparida@soa.ac.in

Tel. No. +91-674-2379425, Fax. +91-6 74-2581637

Materials & Experimental Procedure

Chemicals:

$Ce(NO_3)_3.6H_2O$, $FeCl_2.4H_2O$, sodium carbonate, sodium hydroxide, sodium borohydrate, potassium hydroxide, ammonium chloride, sodium hypochlorite solution (4% w/v) tri-sodium citrate dehydrate, salicylic acid, sodium nitro ferricyanide dehydrate, hydrochloric acid, hydrazine monohydrate, ethanol, and sodium sulphate were purchased from Merck India. Sodium hypophosphite and Nafion solution was purchasaed from sigma Aldrich. All the chemicals were used as received without further purification. Throughout the experiments doubly distilled water was used.

Sample Preparation:

CeO_2 nanosheets were prepared by the method reported in our previous papers [1, 2]. The binary hybrid CeO_2-FeB/P was prepared by dispersing 50 mg of CeO_2NS in a round bottom flask containing 20 mL of water. Then calculated amount of ferrous chloride solids were further

dissolved in the CeO_2 suspension under nitrogen purging condition in ice cold water bath. Then 1 M of solution containing sodium borohydride in potassium hydroxide was injected into the flask and stirred for another 2 h. Then the precipitates were collected and washed with distilled water and kept in a vacuum oven for further use. The different weight percentage of FeB was loaded by varying the iron salt content and sodium borohydride to the CeO_2. And the weight content was adjusted for CeO_2 to FeB as1:1 (CeO_2-FeB1), 1:0.5 (CeO_2-FeB2), 1:0.25 (CeO_2-FeB3) and 1:0.125 (CeO_2-FeB4). To obtain CeO_2-FeB/P, the resulting CeO_2-FeB product was taken in a quartz boat and NaH_2PO_2 were taken in a another quartz and the first boat was placed at the downstream section and the second boat was placed at the upstream section of the quartz tube in the furnace. The resultant solid was annealed in N_2 at 300 °C for 3 h, at a ramping rate of 2 °C min^{-1}. Further, the obtained product was washed with distilled water and, ethanol and dried in vacuum oven at 60 °C. Further, the calcined CeO_2-FeB samples were prepared by the same above discussed method in tubular furnace without using phosphorous source. There is no potential significant hazard associated with this work.

Materials Characterization:

The X-ray diffraction patterns were obtained by Rigaku Miniflex XRD instrument with a monochromator equipped with Cu (Kα) radiation (λ=0.15418 nm) having voltage 40 kV and current of 40 mA from 10˚ to 70˚ at a scan rate of 5˚/min. The TEM and HRTEM images were taken from a Philips TECNAI G^2 electron microscope operated at an accelerating voltage of 200 kV. XPS characterization was carried out in ESCA+, (omicron nanotechnology, Oxford Instrument Germany) equipped with Al Kα X-ray monochromatizating source and binding energy of C1s core (284.6 eV) was taken as reference. UV-visible diffuse reflectance spectrum was taken out from JASCO V-750

spectrophotometer in the range of 200 to 800 nm. The photoluminescence properties were evaluated by JASCO FP-8300 spectrofluorimeter with an excitation wavelength of 340 nm.

Phototelectrochemical analysis:

Photoelectrochemical studies were carried out on IVIUM n STAT electrochemical workstation equipped with a standard three electrode cell and a 300 W Xe lamp. The working electrodes were prepared by a dip coating technique using slurry containing 5 mg catalyst, 700 μL ethanol and 19 μL 1% Nafion solution and then coated it on the surface of FTO. The counter and reference electrodes were Pt electrode and Ag/AgCl. The Mott-Schottky measurement was obtained at 500 Hz in 0.5 M Na_2SO_4 solution under dark condition. However, the Nyquist plot was done at 10^6 Hz to 10^2 Hz at zero bias in the presence of light at open circuit potential.

Photoelectrochemical nitrogen reduction reaction (PEC-NRR) reaction setup:

PEC-NRR was carried out in a gas tight single compartment quartz cell filled with N_2 saturated aqueous electrolyte and equipped with three electrodes containing FTO supported nanoparticles photoelectrode as working electrode. The experiment was investigated with continuous N_2 bubbling and an applied negative potential to the working electrode. The photo reactor was placed in the water bath to maintain the reaction temperature constant and to avoid the thermal effect arises due to light irradiation. All the experiments were carried out at room temperature and pressure. Further, a 300 W Xe lamp was used as light source and illumination intensity near the photoelectrode was calculated to be 113 mW/cm^2 at a fixed distance of 10 cm. To observe the PEC NRR activity over our synthesized materials, we performed chronoamperometry analysis over different photovoltage (-0.6 to -1.4 V vs Ag/AgCl) in N_2 saturated electrolyte such as 0.5 M Na_2SO_4, 0.5 M HCl, and 0.5 M NaOH for

1h. And obtained products are analyzed through Indo-blue phenol method and Wattson Crips method.

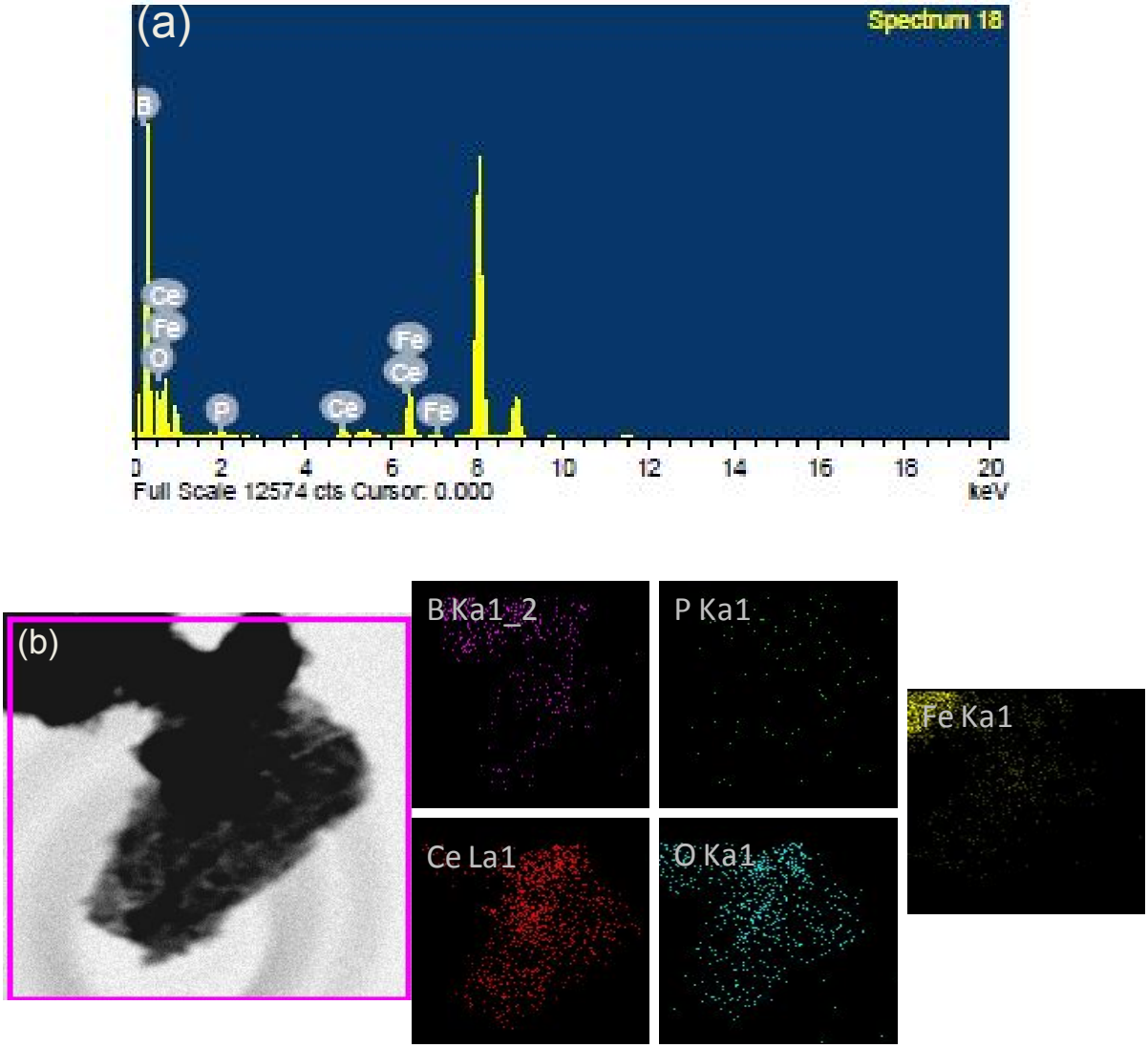

Figure S1 (a) and (b) EDX pattern and colour electron mapping of CeO_2-FeB/P.

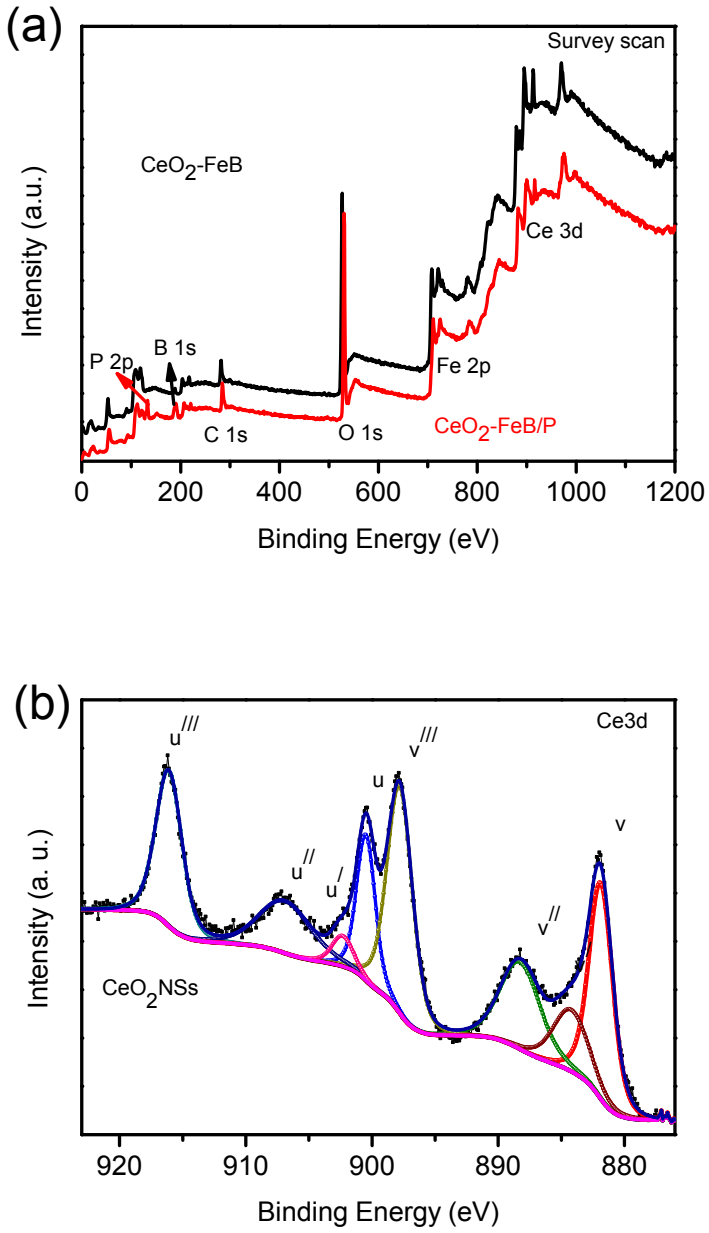

Figure S2 XPS survey spectrum of CeO_2-FeB and CeO_2-FeB/P (a); and High resolution deconvulated Ce3d spectrum of neat CeO_2 (b) "Reproduced with permission from (ref. no.2). Copyright (2018 Royal Society of Chemistry)."

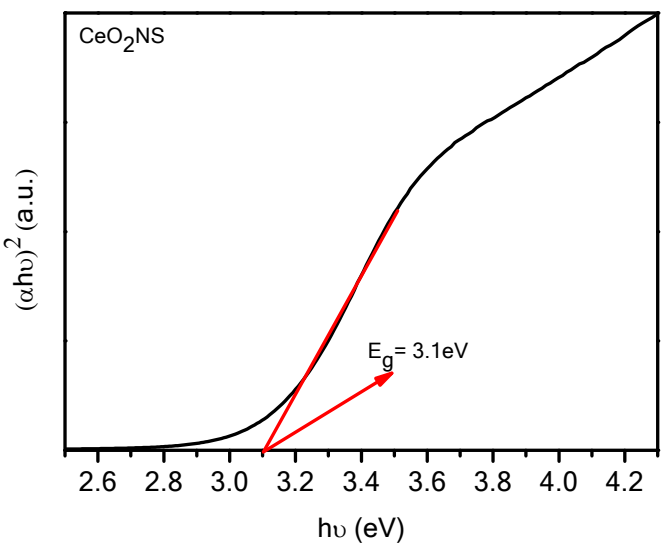

Figure S3 Tauc plot of neat CeO_2 nanosheets.

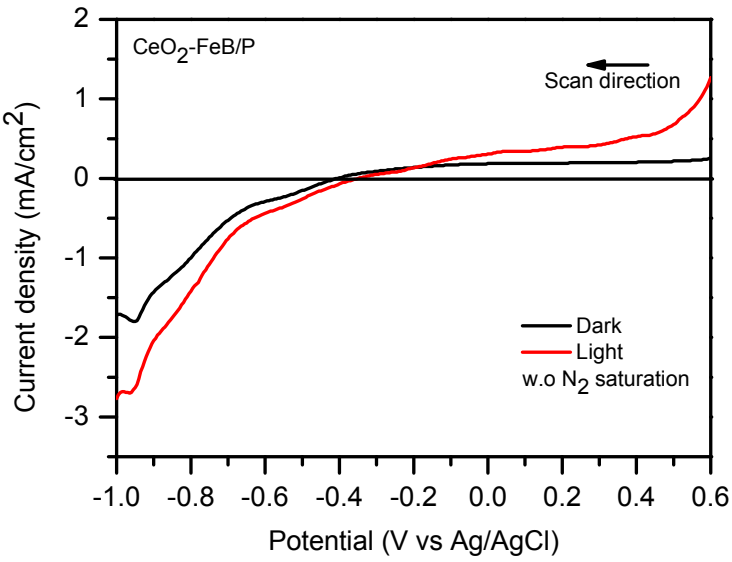

Figure S4 LSV curve of CeO_2-FeB/P in without N_2 saturation environment.

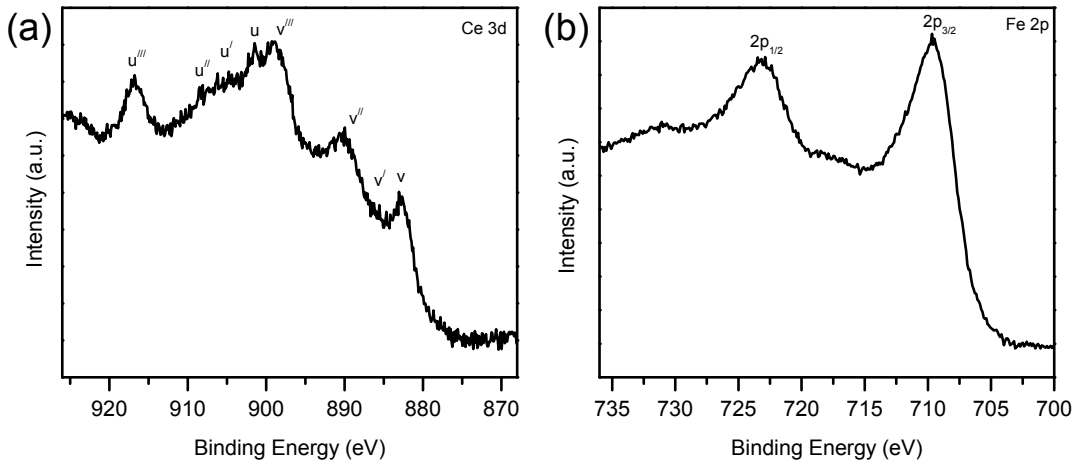

Figure S5 Post PEC XPS spectra of Ce3d and Fe2p of CeO_2-FeB/P.

Table S1 Current state-of the art photoelectrocatalysts for PECNRR.

Photoelectrocatalyst	Reaction Condition	Ammonia Yied	Ref.
$MoSe_2$@g-C_3N_4 micro/nanostructures	N_2-saturated 0.1 M KOH	7.72 μmolh $^{-1}$cm^{-2} FE 28.91% @−0.3 V vs. RHE	3
g-C_3N_5/BiOBr	HCl + Na_2SO_4 solution	29.4 μgh^{-1}mg^{-1} FE 11% @ -0.2 V	4
Au nanoparticles Fe-$W_{18}O_{49}$ nanorods	N_2-saturated Na_2SO_4	9.82 μgh^{-1}cm^{-2} @ -0.65 V vs. Ag/AgCl	5
Mo_2C/C heterostructure	N_2-saturated lithium sulfate solution	6.6 μgh^{-1}mg^{-1} FE 37.2% @0.2 V vs. Ag/AgCl	6
Au-Ag_2O nanocages	N_2-saturated DI water	28.2 mgm^{-2}h^{-1} solar-to-ammonia conversion efficiency 0.017%	7
BiOI photocathode $BiVO_4$ anode	N_2-saturated water	1.4 2 mmolm^{-2}h^{-1} @0.4 V vs RHE	8
Ag/bSi photocathode	N_2-saturated Na_2SO_4	2.87 μmolh^{-1}cm^{-2} FE 40.6% @ -0.2 V vs. RHE	9
TiO_2 layer on plasmonenhanced rutile TiO_2/Au nanorods	N_2-saturated water	13.4 nmolcm^{-2}h $^{-1}$ under 1 sun illumination	10
$SrTiO_3$/AuNPs/Zr/ZrOx thin film	anodic chamber-KOH, cathodic chamber-HCl-N_2	6.5 nmolh $^{-1}$cm^{-2}	11
MoS_2@TiO_2	N_2-saturated Na_2SO_4	1.42 μmol h^{-1}cm^{-2}	12

		FE 65.52% @ @ -0.2 V vs. RHE	
CuO and Cu_2O photocathodes	$^{15}N_2$-saturated KOH	FE 17% and 20% @0.6 and 0.4 V vs RHE	13
Black phosphorus (BP) nanosheet	N_2-saturated HCl	102.4 μg h^{-1} $mgcat^{-1}$ FE 23.3% @ −0.4 V vs. RHE	14
H-terminated B doped diamond	anodic chamber-KI, cathodic chamber-N_2-saturated water	1.8 μgh^{-1}	15
CeO_2-FeB/P	N_2-saturated Na_2SO_4	9.54 $\mu gcm^{-2}h^{-1}$ Solar-to-ammonia conversion efficiency of 0.046% @-0.12 V vs RHE	This work

References:

1) Dai, Q.; Bai, S.; Li, H.; Liu, W.; Wang, X.; Lu, G. Template-free and non-hydrothermal synthesis of CeO_2 nanosheets via a facile aqueous-phase precipitation route with catalytic oxidation properties. *CrystEngComm*. 2014, *16* (42), 9817-9827.
2) Sultana, S.; Mansingh, S.; Parida, K. Rational design of light induced self healed Fe based oxygen vacancy rich CeO_2 (CeO_2 NS–FeOOH/Fe_2O_3) nanostructure materials *J. Mater. Chem. A* 2018, *6* (24), 11377-11389.
3) Mushtaq, M.A.; Arif, M.; Fang, X.; Yasin, G.; Ye, W.; Basharat, M.; Zhou, B.; Yang, S.; Ji, S.; Yan, D. Photoelectrochemical reduction of N_2 to NH_3 under ambient conditions through hierarchical $MoSe_2$@gC_3N_4 heterojunctions. *J. Mater. Chem. A* 2021, *9* (5), 2742-2753.
4) Li, M.; Lu, Q.; Liu, M.; Yin, P.; Wu, C.; Li, H.; Zhang, Y.; Yao, S. Photoinduced charge separation via the double-electron transfer mechanism in nitrogen vacancies g-C_3N_5/BiOBr for the photoelectrochemical nitrogen reduction. *ACS Appl. Mater. Interfaces* 2020, *12* (34), 38266-38274.

5) Vu, M.H.; Nguyen, C.C.; Do, T.O. Synergistic Effect of Fe doping and plasmonic Au nanoparticles on $W_{18}O_{49}$ nanorods for enhancing photoelectrochemical nitrogen reduction. *ACS Sustain. Chem. Eng.* 2020, *8* (32), 12321-12330.

6) Li, X.; Fan, W.; Xu, D.; Ding, J.; Bai, H.; Shi, W. Boosted photoelectrochemical N_2 reduction over Mo_2C in situ coated with graphitized carbon. *Langmuir* 2020, *36* (48), 14802-14810.

7) Nazemi, M.; El-Sayed, M.A. Plasmon-enhanced photo (electro) chemical nitrogen fixation under ambient conditions using visible light responsive hybrid hollow Au-Ag_2O nanocages. *Nano Energy* 2019, *63*, 103886.

8) Bai, Y.; Bai, H.; Qu, K.; Wang, F.; Guan, P.; Xu, D.; Fan, W.; Shi, W. In-situ approach to fabricate BiOI photocathode with oxygen vacancies: Understanding the N_2 reduced behavior in photoelectrochemical system. *Chem. Eng. J.* 2019, *362*, 349-356.

9) Wang, B.; Yao, L.; Xu, G.; Zhang, X.; Wang, D.; Shu, X.; Lv, J.; Wu, Y.C. High-efficient photoelectrochemical synthesis of ammonia using plasmon-enhanced black silicon under ambient conditions. *ACS Appl. Mater. Interfaces* 2020, *12* (18), 20376-20382.

10) Li, C.; Wang, T.; Zhao, Z.J.; Yang, W.; Li, J.F.; Li, A.; Yang, Z.; Ozin, G.A.; Gong, J. Promoted fixation of molecular nitrogen with surface oxygen vacancies on plasmon-enhanced TiO_2 photoelectrodes. *Angew. Chem. Int. Ed.* 2018, *57* (19), 5278-5282.

11) Oshikiri, T.; Ueno, K.; Misawa, H. Selective dinitrogen conversion to ammonia using water and visible light through plasmon-induced charge separation. *Angew. Chem.* 2016, *128* (12), 4010-4014.

12) Ye, W.; Arif, M.; Fang, X.; Mushtaq, M.A.; Chen, X.; Yan, D. Efficient photoelectrochemical route for the ambient reduction of N_2 to NH_3 based on

nanojunctions assembled from MoS_2 nanosheets and TiO_2. *ACS Appl. Mater. Interfaces* 2019, *11* (32), 28809-28817.

13) Jang, Y.J.; Lindberg, A.E.; Lumley, M.A.; Choi, K.S. Photoelectrochemical nitrogen reduction to ammonia on cupric and cuprous oxide photocathodes. *ACS Energy Lett*. 2020, *5* (6), 1834-1839.

14) Liu, D.; Wang, J.; Bian, S.; Liu, Q.; Gao, Y.; Wang, X.; Chu, P.K.; Yu, X.F. Photoelectrochemical synthesis of ammonia with black phosphorus. *Adv. Funct. Mater*. 2020, *30* (24), 2002731.

15) Zhu, D.; Zhang, L.; Ruther, R.E.; Hamers, R.J. Photo-illuminated diamond as a solid-state source of solvated electrons in water for nitrogen reduction. *Nature Mater*. 2013, *12* (9), 836-841.